Nanoscale

Insights into the Copolymerization of Metal-Organic Nanotubes from Ligand Mixtures Using Small Angle Neutron Scattering

Journal:	*Nanoscale*
Manuscript ID	NR-ART-11-2024-004820.R2
Article Type:	Paper
Date Submitted by the Author:	25-Apr-2025
Complete List of Authors:	Haque, Md Ashraful; The University of Tennessee Knoxville, Chemistry Barrett, Jacob; The University of Tennessee Knoxville, Chemistry Carroll, Xian; The University of Tennessee Knoxville College of Arts and Sciences Jenkins, David; The University of Tennessee Knoxville, Department of Chemistry Dadmun, Mark; The University of Tennessee Knoxville, Chemistry

Insights into the Copolymerization of Metal-Organic Nanotubes from Ligand Mixtures Using Small Angle Neutron Scattering

Md Ashraful Haque, Jacob A. Barrett, Xian B. Carroll, David M. Jenkins,* and Mark D. Dadmun*

Department of Chemistry, University of Tennessee, Knoxville, Tennessee 37996, United States

Abstract

Metal-organic nanotubes (MONTs) are porous, tunable 1D nanomaterials akin to metal-organic frameworks (MOFs). MONTs are synthesized *via* metal salts and coordinating ligands akin to MOFs, but crucially they are anisotropic, unlike most MOFs. Recently, MONTs have been shown to form statistically random copolymers, however their mechanism of growth remains largely unexplored. Full realization of the potential of MONTs necessitates thorough understanding of the mechanism of MONT growth. Herein, small-angle neutron scattering (SANS) was employed to investigate the copolymerization mechanism of two 1,2,4-ditriazole ligands and to quantify the inclusion of solvent within the MONT pore. The results show parallelepiped-shaped structures initially formed, which then aggregate to form larger lamellar structures. Additional experimentation with a deuterated ligand showed the reactivities of all ligands are approximately equal, causing random ligand distribution within the resulting MONT. Finally, the results quantify the amount of solvent incorporated within the nanostructure pores at different stages of the formation process. These results show that early in the reaction the MONTs contain *ca* 45% solvent and contain *ca* 55% solvent late in the reaction when the MONTS a nearly fully formed.

Introduction

Metal-organic nanotubes (MONTs) are a class of crystalline, porous, and tunable materials that are formed from a metal salt and a suitable organic bridging ligand.[1, 2] Grown in solvothermal conditions, MONTs share many of the properties of their 3D counterparts, metal-organic frameworks (MOFs), including the incorporation of multiple ligands within a single structure, or ligand multivariance, akin to copolymerization in traditional polymers.[2-6] Unlike virtually all MOFs, MONTs are anisotropic, with the main dimension of growth lying along the length of the tube, resulting in potential applications that take advantage of their anisotropy, such as nanostraws, ion exchange materials, and nanowires.[7-12] The dimensional control of materials at a molecular level provides the opportunity to tune the properties and applications of the material.[12-16] However, MONT development at this level is still in its infancy due to a lack of detailed understanding of MONT growth and assembly.

Moreover, there remain quite a few uncertainties regarding the assembly and structure of the MONT. For instance, while it is understood that gases and solvents can penetrate the MONT, there are few analytical methods to directly measure the amount of solvent within a MONT. Additionally, structural models have not yet been developed that account for multi-ligand MONT growth over nanoscale ranges. Formation of MONTs have been studied *in-situ via* SANS and *ex-situ via* numerous techniques.[6, 16-19] These studies show double-hinged ditriazole MONTs form isotropic microcrystalline species, which then aggregate as the rate-limiting step and grow preferentially in one dimension. While previous *in-situ* studies have suggested a copolymerization-like process, there are no examples to date that measure the distribution of solvent within a MONT *in situ*.[17] To accurately predict and utilize the properties of multi-ligand MONTs, where one ligand can impart

unique functionality into the resulting material, MONT growth and aggregation from ligand mixtures must be understood.

Small angle neutron scattering (SANS) is a useful technique that investigates the structure and assembly of materials over length scales from 10-1500 Å, and has been used previously to investigate the growth process of various MOF and MONT architectures.[17, 19-22] The formation process of hinged 1,2,4-ditriazole multi-ligand MONTs was previously investigated with (4,4′-(1,3-(xylene)-diyl) bis(1,2,4-triazole)) (**L1**) and 4,4′-((5-methyl-1,3-phenylene)bis-(methylene))bis(4H-1,2,4-triazole) (**L2**) *via* SANS.[17] Under solvothermal conditions, **L1** and copper(II) bromide in dimethylformamide (DMF) form a 1D MONT, while **L2** forms a 2D stair-stepped coordination polymer (**Figure 1A**). Despite the dissimilar structures, the growth of mixtures of **L1** and **L2** ligands mimic that of pure **L1** MONT, implying **L1** influences the orientation of **L2** within the growing crystal and can produce a 1D MONT (**Figure 1B**).

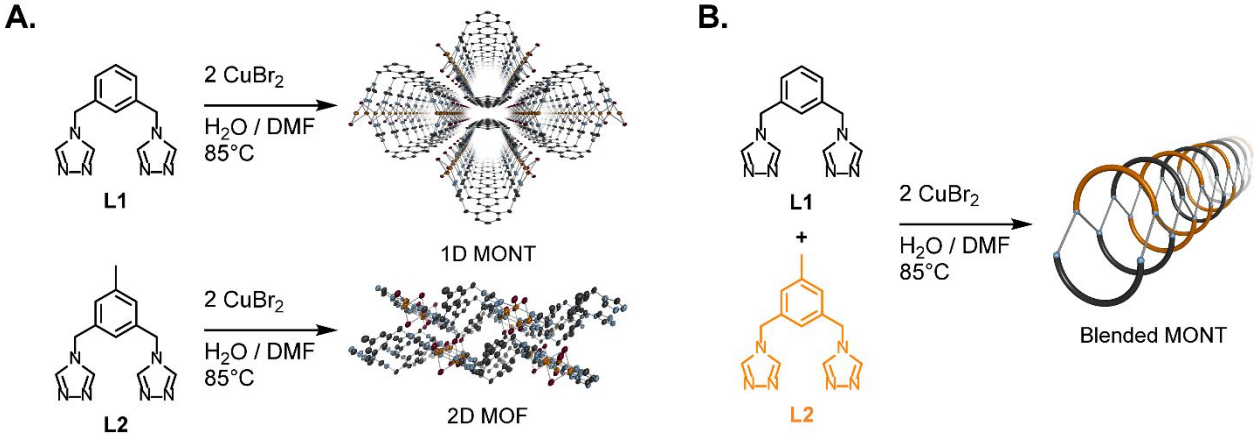

Figure 1. Synthetic schemes of **L1** – **L2** copolymerization. (A) Whereas 1,2,4-ditriazole ligand **L1** forms a 1D MONT under solvothermal conditions, 1,2,4-ditriazole ligand **L2** forms a stair-stepped 2D MOF under identical reaction conditions.).[12,17] (B) Copolymerization of **L1** and **L2** yield a mixed-ligand nanotube with the structure dominated by **L1**.).[17]

The previous study was unable to explicitly monitor the distribution of ligands within the growing MONT. As neutron scattering is dominated by the scattering of hydrogen atoms in

organic materials, the deuteration of one ligand provides the contrast necessary to determine the distribution of the deuterated ligand within a mixture of protonated and deuterated structures. The reactivity ratio of two components in a copolymerization reaction is the ratio of the rate constant for the addition of one component to a component of the same type to the rate constant for the addition of the other monomer to that same reaction site.[23] In this manuscript, we utilize **L1**, **L2**, and a contrasting deuterated analog of **L1** (**L1-*d*$_8$**, **Figure S1**) to measure the distribution of ligands **L1** and **L2** in synthesized MONTs to simultaneously offer semi-quantitative insight into the relative reactivity of the two ligands and quantify the amount of solvent incorporated into the final MONT structure *via* SANS.

Experimental

Quantifying the distribution of the deuterated ligand **L1-*d*$_8$** in the copolymeric MONTs provides insight into the copolymerization process of **L1** and **L2** in the final nanostructure. Therefore, **L1-*d*$_8$** was synthesized (see **ESI**) and reacted with **L1** at different protonated/deuterated ratios 100:0, 80:20, 60:40, 40:60 (100 **L1**: 0 **L1-*d*$_8$**). Deuterium incorporation was determined to be a minimum of 95% in 8 of 12 possible hydrogen *via* ^{1}H NMR (see **Figure S3**). Further experiments were performed to investigate the distribution of ligands in the copolymerization of **L1** and **L2** ligand by monitoring the structure of MONTs formed from mixtures of **L1**, **L1-*d*$_8$**, and **L2** at different ratios 50:0:50, 35:15:50, 25:25:50, 15:35:50, 0:50:50 (**L1**: **L1-*d*$_8$**: **L2**). To corroborate L1 and L2 ratios within the final ligand, bulk-scale reactions were performed at **L1**, **L1-*d*$_8$**, and **L2** ratios of 50:0:50, 35:15:50, 25:25:50, 15:35:50, and 0:50:50 and subjected to acid digestion.

SANS Measurement and Analysis

Small angle neutron scattering measurements were performed at the Oak Ridge National Laboratory on the general purpose SANS (CG2 GP SANS) at HFIR. Previous studies showed that approximately 8-10 hours is required to complete the reaction for the formation of a MONT.[17] Hence, SANS measurements were taken immediately after the addition of ligands into the $CuBr_2$ solution and 10 hours after the initial measurements. Moreover, SANS measurements of a 33:67 mixture of deuterium oxide (D_2O) and deuterated dimethyl formamide (DMF-d_7) were also obtained. The scattering of the samples was measured at two detector distances that cover the Q ranges from 0.0039 to 0.20 $Å^{-1}$. Here, Q is the momentum transfer which is defined as $Q = 4\pi \sin \theta/\lambda$, where λ is the neutron wavelength and θ is the scattering angle. The coherent scattering profile of all the samples were obtained after accounting for empty cell scattering, sample cell thickness, sample transmission and solvent scattering. SasView software package was used to analyze the scattering profiles of the MONT samples.[24]

Our previous study investigated the reaction of **L1** and **L2** with copper bromide to form nanoscale materials.[17] To confirm the phase purity of 50:50 **L1:L2**, powder X-ray diffraction (PXRD) was performed as shown in **Figure S2**. A post-synthetic blending of **L1** MONT and **L2** MOF resulted in two sets of peaks, most notably at approximately 9 2θ, whereas the MONT formed from the 50:50 **L1**:**L2** exhibited only one set of peaks, signifying the resulting material is pure single phase.[6] Additionally, the PXRD pattern of 50:50 **L1**:**L2** exhibited high symmetry, unlike the **L2** MOF, and the peak positions of 50:50 **L1:L2** agree well with that of **L1** MONT, suggesting the material formed is isostructural to **L1** MONT.

With the 100:0 and 50:50 **L1**:**L2** structures established, a parallelepiped model was initially chosen to analyze the MONT scattering profile. However, the parallelepiped model failed to capture the low-q scattering profile as shown in **Figure S8**. This indicates that MONT forms

structures at two different length scales when formed from both the pure **L1** and mixture of **L1** and **L2** ligands. To capture the whole scattering profile, a combined model that includes the scattering of a parallelepiped and a lamella was chosen. A combination of both models resulted in successfully fitting the scattering profile of MONTs formed from pure **L1**, mixtures of protonated and deuterated ligand **L1** and ternary mixtures of **L1**, deuterated **L1**, and **L2** ligands. During the fitting process, the polydispersity (PD) of the lamellar model that considers the distribution of thickness of lamellae was included for robust fitting of the scattering profiles of all MONT samples.

Discussion and Results

Estimating solvent entrapped in the MONTs

Small angle neutron scattering provides data that can be analyzed to elucidate the formation process of nanotubes from mixtures of protonated and deuterated ligand **L1**. **Figure 2** shows the scattering profiles that emerged from the reaction of varying compositions of protonated and deuterated **L1** ligand and the copper (II) bromide at 0 hr. and 10 hrs. **Equation 1** provides the relationship between the scattered intensity and the structure of the evolving nanostructure.

$$I(Q) \sim \Delta\rho^2 \times c \times F(Q) \times S(Q) \qquad \mathbf{1}$$

In **Equation 1**, F(Q) is the form factor that correlates to the shape of the structure of the MONT, S(Q) is the structure factor that details the particle-to-particle interactions, and, in this case, since the MONT solution is dilute, S(Q) = 1. In **Equation 1**, $\Delta\rho^2$ is the difference in the scattering length density of the deuterated solvent and the MONT formed from the mixture of protonated and deuterated ligands. The scattering length density (SLD) of each species can be calculated from its density and atomic composition. Using the NIST activation calculator, the SLD of pure MONT from **L1**, of the pure nanostructure from **L2**, of the pure MONT from **L1-d$_8$**, and of the solvent, a 33:67 mixture of D_2O and DMF-d_7, are calculated to be 2.80 x 10^{-6} Å^{-2}, 2.65 x 10^{-6} Å^{-2} 4.72 x 10^{-6} Å^{-2} and 6.0 x 10^{-6} Å^{-2} respectively.[25]

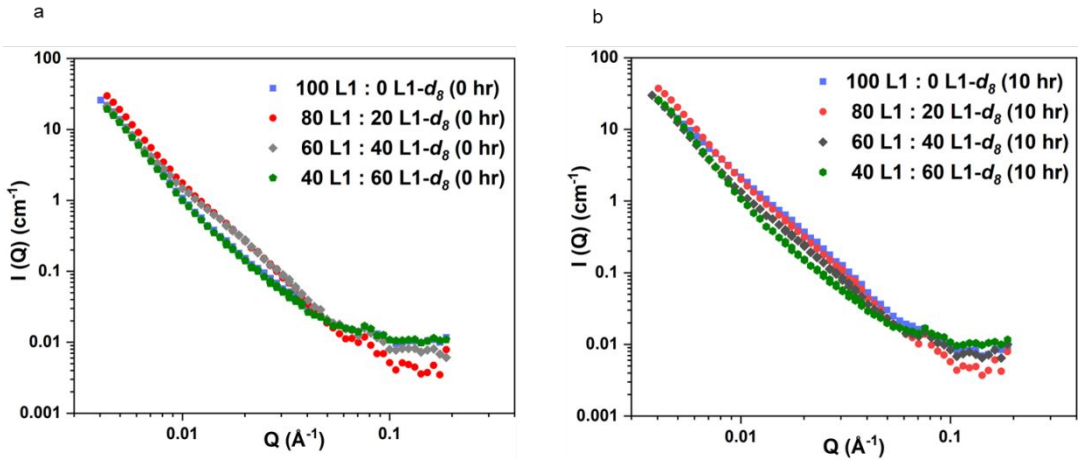

Figure 2. Small angle neutron scattering profiles of MONT formed from **L1**:**L1-*d*$_8$**. at ratios of 100:0, 80:20, 60:40,40:60 at (a) 0 hr. and (b) 10 hrs.

The addition of **L1-*d*$_8$** to the mixture of **L1** will decrease the amount of protons in the MONT structure and will decrease neutron scattering contrast between the MONT and deuterated solvent, $\Delta\rho^2$. Consequently, the intensity of the neutron scattering profile of the MONT should decrease proportional to the amount of deuterated **L1-*d*$_8$** added to the mixture. However, only modest decreases in intensity are observed (**Figure 2**) with an increase of **L1-*d*$_8$** in the mixture, where any changes are not proportional to the amount of deuterated ligand in the reaction mixture.

The limited decrease in scattering intensity can be explained by the fact that the MONT scattering object is not the pure MONT, but that the MONT is imbued with deuterated solvent. In fact, previous studies showed that DMF solvent incorporates into the pores of a MONT structure.[12, 17] The limited decrease in scattering intensity with the addition of deuterated **L1** ligand into the reaction mixture is consistent with the incorporation of deuterated solvent into the pores of the MONT structure, as the SLD of the MONT + deuterated solvent will be greater than that of the MONT itself.

In fact, fitting the scattering profile to the combined model provides the scattering length density (SLD) of the MONT + solvent mixture, offering a unique analytical method to quantify the amount of deuterated solvent incorporated into the MONT pores. The experimental SLD of the MONT is obtained by fitting the 100 **L1**:0 **L1-*d*$_8$** scattering profile at 0 hr. and 10 hrs. to the combined model of lamellar and parallelepiped, as shown in **Figure S9**. The successful fitting of the scattering profile provides the SLD of the MONT ~4.20 x 10^{-6} Å^{-2} (lamellae) and 4.12 x 10^{-6} Å^{-2} (parallelepiped). **Equation 2** provides the mathematical relationship between the amount of deuterated solvent incorporated in the MONT, Φ_1, the measured scattering length density of MONT that includes the solvent and of the solvent.

$$\emptyset_1 = \frac{SLD\ of\ MONT_{experimental} - SLD\ of\ MONT_{theoretical}}{SLD\ of\ Solvent_{theoretical} - SLD\ of\ MONT_{theoretical}} \qquad \mathbf{2}$$

Determining the amount of solvent in the MONT/solvent complex from **Equation 2** shows that the MONT/solvent complex consists of ~45% solvent at 0 hr. and ~55% solvent at 10 hrs. The quantitative measure of the amount of deuterated solvent imbued into the MONT indicates that solvent incorporation into the MONT structure occurs quickly after the reaction between the salt and ligand occurs. It appears that further refining of the MONT structure with reaction time

provides opportunities to further increase the amount of solvent in the MONT structure. From a broader perspective, however, this analysis also emphasizes that a significant amount of solvent is incorporated in the nanotube structure, which can impact the amount of MONT surface area that is available for penetration and adsorption by adsorbents and reactants.

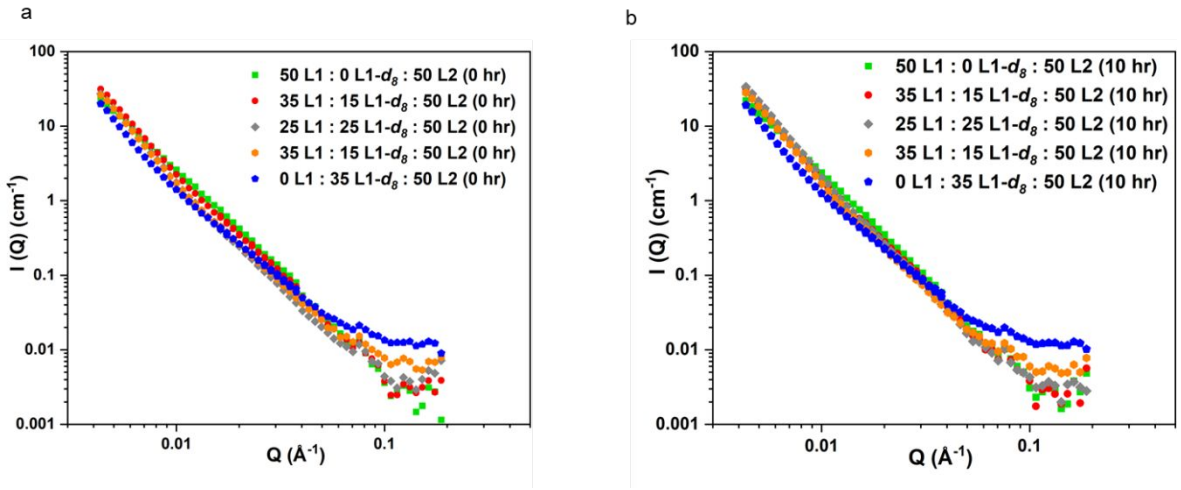

Figure 3. Small angle neutron scattering profile of MONT formed from **L1**: **L1-*d*$_8$**: **L2** at ratios of 50:0:50, 35:15:50, 25:25:50, 15:35:50, 0:50:50 at (a) 0 hr. and (b) 10 hrs.

Similar to the scattering profiles of the nanostructure obtained from the mixtures of protonated and deuterated **L1**, the scattering profiles of the mixtures of **L1**, **L2** and **L1-*d*$_8$**, presented in **Figure 3** (a and b), also shows minimal decrease in intensity with the incorporation of deuterated **L1** in the mixture. Hence, a similar analysis of the change in SLD of the MONT/solvent complex using **Equation 2** also provides the amount of solvent in the MONT structure formed from the 50 **L1**: 50 **L2** mixtures. In these analyses, the scattering profiles of the 50 **L1**: 50 **L2** nanostructures are fit to the combined lamellar and parallelepiped model to obtain the SLD of the nanostructures formed from the reaction between the metal salt and the ligands, **L1** and **L2 as shown in Figure S10**. Using **Equation 2**, the solvent incorporated into the MONT structure is found to be ~45% at 0 hr. and ~55% at 10 hrs. The amount of solvent incorporated into the mixture of **L1** and **L2** ligand at the initial and final stages of the reaction is similar to the

amount incorporated into MONT/solvent complex formed from **L1** ligand. This result suggests that incorporating the **L2** ligand into the MONT structure does not significantly alter the ability of the solvent to penetrate the MONT and fill nanopores.

Evolution of nanotube formation

The fitting process of the scattering profile of **L1** and **L1-*d*$_8$** mixtures as well as the **L1**, **L1-*d*$_8$**, and **L2** mixtures required a combined model fit that includes a larger lamellae shaped nanostructure and a smaller parallelepiped shaped nanostructure. **Figure 4** shows an illustration of the lamellar structure that correlates to the larger length scale nanostructure, which has a finite thickness, but its dimensions in the other two dimensions are larger than the SANS experiment can monitor. Thus, the lamella width and length are considered 'infinite', but the parallelepiped structure dimensions are on a smaller length scale that has thickness, length, and width (A, B, and C in **Figure 5**) that are within the resolution of the SANS experiment.

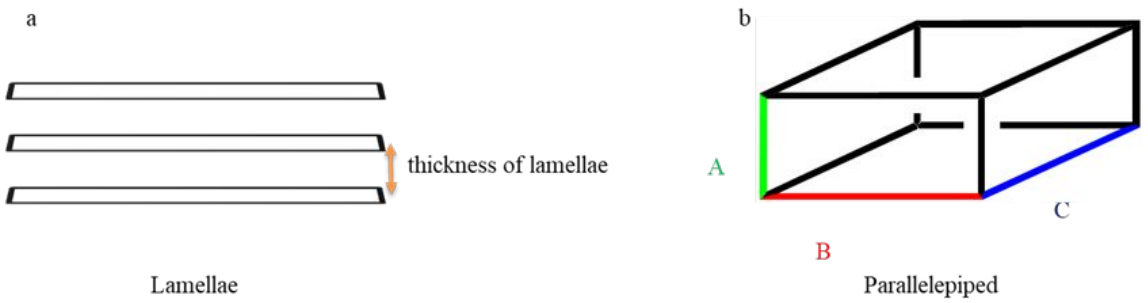

Figure 4. Illustration of lamellae formed from the aggregatation of smaller parallelepiped shaped MONTs. (A) Inifitely large sheets (lamelllae) formed with one dimension suitable for SANS measurements. (B) Three dimension of parallelepiped-shaped structure where A is the thickness, B is the width and C is the length.

We initially consider the lamellae to be a larger structure that consists of parallelepiped building blocks. A previous study of the assembly of similar triazole ligand-based MONT structures showed the formation of larger 3D MONT structures from smaller MONT

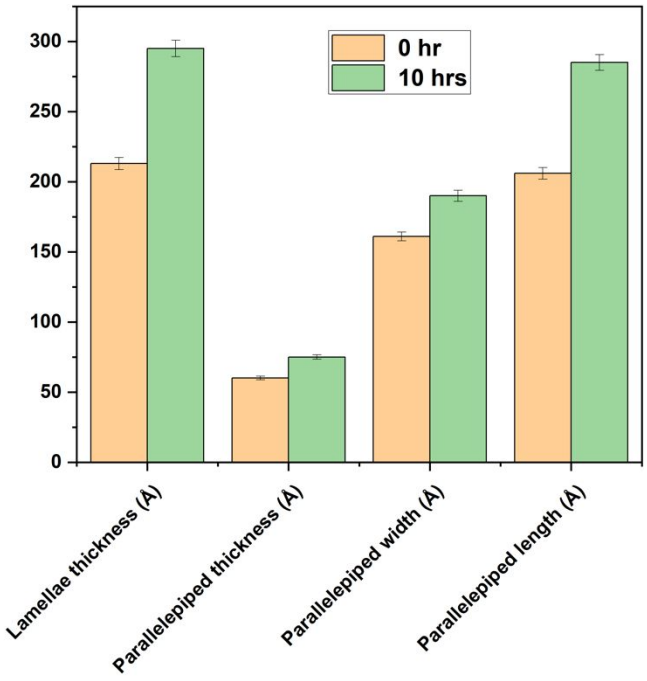

Figure 5. Change in thickness of lamellae of MONT and change in thickness, width and length of parallelepiped MONT formed from **L1** at 0 hr and 10 hrs.

nanostructures. To more fully understand the growth formation of MONTs from **L1** ligand, the time evolution of the thickness of the MONT lamellae and the thickness, width and length of the parallelepiped building block were carefully analyzed. The fitting of scattering profile of the 100:0, 80:20, 40:60 and 60:40 (**L1**: **L1-*d*$_8$**) samples at 0 hr. and 10 hrs. to the combined model provides this structural information. Initially, the scattering profile of 100:0 **L1**:**L1-*d*$_8$** is fit to the combined model to understand the growth of pure ligand **L1** with reaction time. **Figure 5** documents the thickness of the lamellae and the dimension of parallelepiped that emerge from the fitting of the scattering profile of 100:0 **L1**:**L1-*d*$_8$** ligand mixtures. **Figure 5** shows that the thickness of the MONT lamellae increases from ~213 Å to ~295 Å from the initial reaction to 10 hr. The thickness, width and length of the parallelepiped building block increases from 59 Å to 80 Å, 161 Å to 187 Å and 206 Å to 279 Å respectively over this same time period. This indicates that the parallelepiped shaped MONT structure increases anisotropically in all directions from 0 to 10 hrs. Moreover, one dimension of the parallelepiped building block is similar in length to the thickness of the lamellae after 10hrs (length of parallelepiped = thickness of lamellae = ~300 Å). This suggests that the smaller parallelepiped building blocks aggregate along two faces of the parallelepiped to form an extended large sheet-like lamellar structures. Unfortunately, SANS can only measure length scales of up to ~1500 Å

and thus these experiments can only indicate that the sheet-like aggregates of the MONTs are larger than ~1500 Å.[17]

The scattering profiles of the MONTs formed from the contrast variation experiments which varies the **L1** and **L1-*d*$_8$** composition were also measured. The first approach to fit these scattering curves fixed the thickness of the lamellae as well as the dimensions of the parallelepiped structure to that obtained from fitting the MONT scattering profile of the purely protonated **L1** sample. While this fitting approach provided a robust fit of the data to the model, the polydispersity of the thickness of the lamellae became too large (~ 1.4, which is above the accepted range ($0 < PD \leq 1$).[24] Hence fitting the scattering profiles of the mixed deuterated and protonated **L1** samples allowed the thickness of the lamellae and dimensions of the parallelepiped structures to vary. This approach resulted in polydispersity of the thickness of the MONT lamellae to be within an acceptable range. Using this fitting protocol, **Figure 6** documents the variation in the thickness of the lamellae and the dimensions of the parallelepiped structures in these protonated/deuterated **L1** mixtures as the composition of the protonated and deuterated **L1** varies.

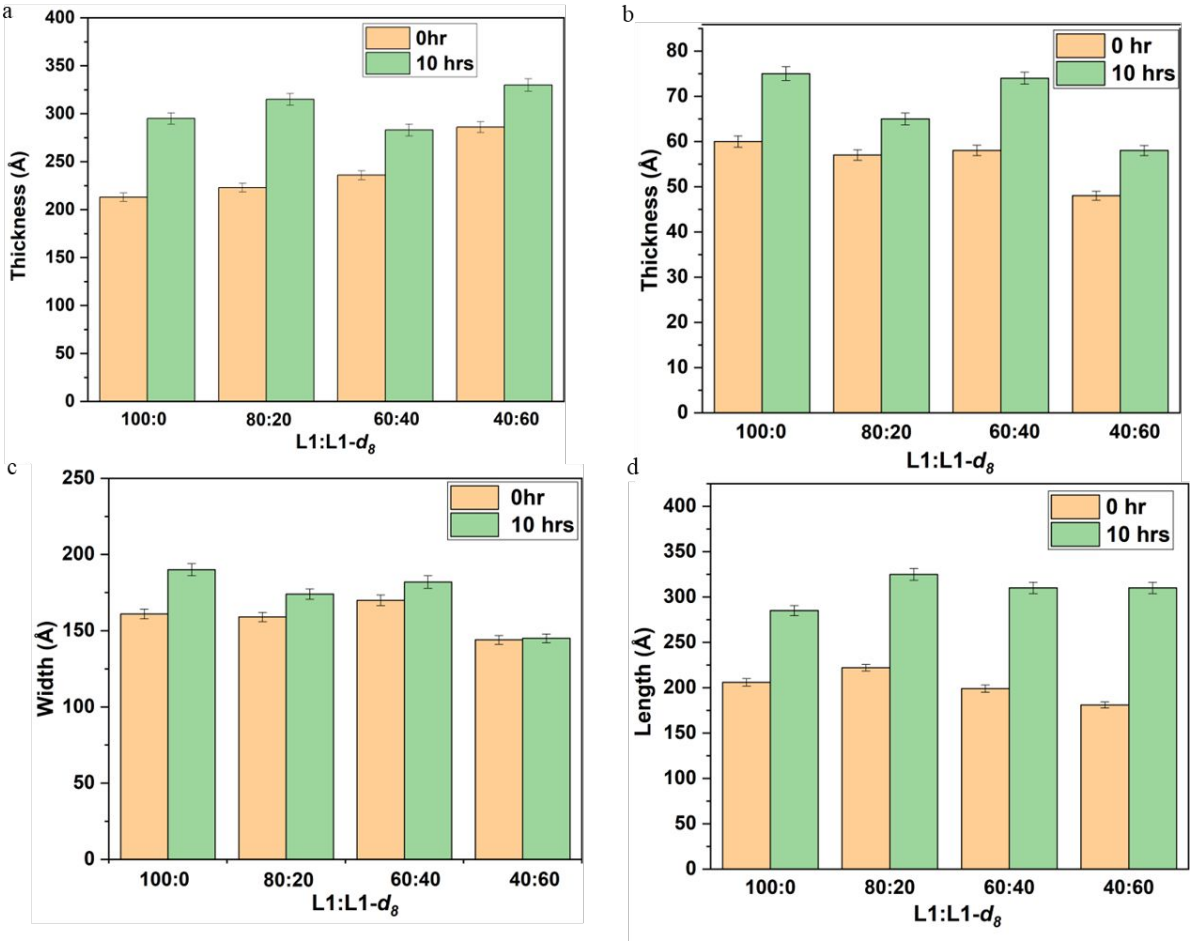

Figure 6. Change in thickness of lamellae MONT and change in thickness, width and length of parallelepiped MONT formed from varying compostion of **L1** and **L1-*d*$_8$** at 0 hr and 10 hrs. (a) Total thickness of the lamellae MONT. (b). Thickness of the parallelepiped MONT. (c) Width of the parallelepiped MONT. (d) Length of the parallelepiped MONT.

The results show that the average thickness of the lamellae is ~240 Å at 0 hr. which increases to a thickness of ~306 Å corresponding to a ~28% increase in thickness of the lamellae at 10 hrs. of reaction. Similarly, the thickness, width and length of the parallelepiped MONT initially averages 56 Å,157 Å and 192 Å respectively, which increases about 23%, 10%, and 59% in thickness, width and length after the reaction between ligand **L1** and copper salt at 10 hrs. This anisotropic increase in three dimensions of the parallelepiped shaped building blocks of the MONTs from mixtures of protonated and deuterated **L1** is consistent with the formation process

of the MONTs created from pure protonated ligand **L1**. Similarly, the length of the smaller parallelepiped and thickness of the larger lamellae are also similar to each other and the length scales of MONTs formed from pure protonated ligand **L1**.

Using a similar fitting model, this combined model is also used to fit the scattering data of the MONTs formed from mixtures of the **L1** and **L2** ligand. Analysis of these scattering curves provides insight into the change in the thickness of the lamellae and dimensions of the parallelepiped formed from mixtures of **L1**, **L1-*d*$_8$** and **L2** at the ratios of 50:0:50, 35:15:50, 25:25:50, 15:35:50, 0:50:50 (**L1**: **L1-*d*$_8$**: **L2**) at 0 hr. and 10 hrs. **Figure 7** shows the thickness of the lamellae and the dimensions of the parallelepiped nanostructures for these samples at early stages of the reaction and after 10 hr. of reaction. The results show that the average thickness of the larger lamellae at 0 hr. is ~ 240 Å which grows to ~ 305 Å at 10 hr. and that the average thickness, width and length of the parallelepiped-shaped nanostructure formed from the mixed **L1** and **L2** ligands at the end of the reaction (10 hrs.) are *ca.* 57 Å, 165 Å and 292 Å respectively.

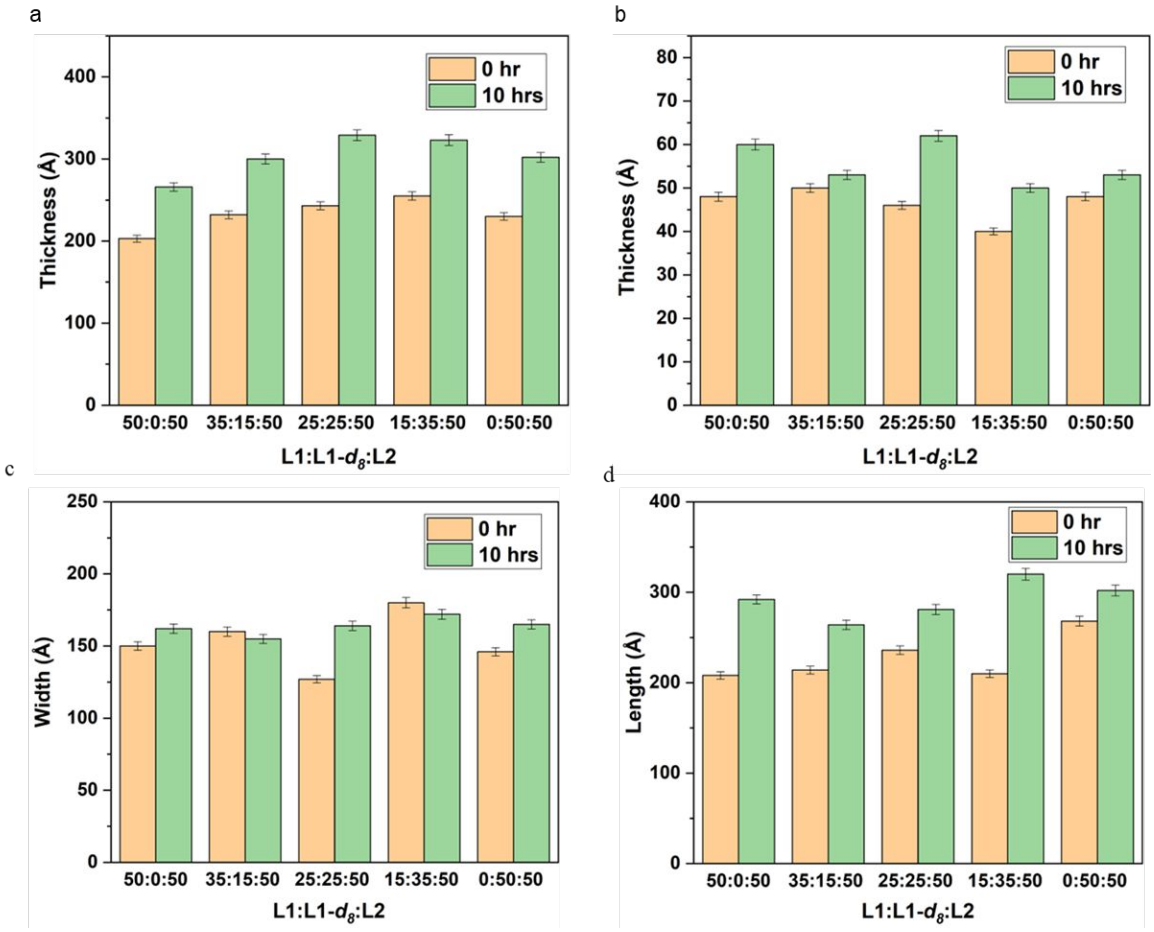

Figure 7. Change in thickness of lamellae MONT and change in thickness, width and length of parallelepiped MONT formed from varying compostion of **L1**, **L1-d_8** and **L2**. (A) Total thickness of the lamellae MONT. (B) Thickness of the parallelepiped MONT. (C) width of the parallelepiped MONT. (D) Length of the parallelepiped MONT.

Comparison of the final thickness of the lamellae nanostructures and the dimensions of the parallelepiped-shaped nanostructures formed from the **L1** and **L2** ligand to that of the pure **L1** ligand indicates that the final nanostructures formed from the **L1** ligand and the mixture of **L1** and **L2** ligand have similar dimensions. A previous study by Shrestha et al. showed that nanostructure formed from the pure **L2** ligand are significantly larger relative to the structures formed from the pure **L1** ligand.[17] Therefore, the similarity in the dimensions of the nanostructure formed from pure **L1** and the mixture of **L1** and **L2** ligands indicates that both parallelepiped-shaped

nanostructures and aggregated parallelepiped or lamellae-like nanostructures are dominated by the assembly of the **L1** ligand.

The copolymerization of nanostructures from ligands L1 and L2

To understand the manner of copolymerization of nanostructures from the reaction between the two ligands and copper salt, the first system studied focused on the nanotube formed from the mixture of protonated and deuterated ligand, **L1** and **L1-*d*$_8$**. Quantifying the dependence of the amount of **L1-*d*$_8$** in the MONTs formed on the reactant feed composition provides insight into the relative reactivity of the deuterated and protonated ligand in the MONT formation reaction. If the reactivities are very similar, the ligands will be randomly distributed in the MONTs and the composition of the formed MONTs will be similar to the feed composition. However, if one ligand is more reactive, the formed MONTs will have a higher composition of that ligand than is in the feed. Quantifying the amount of deuterated ligand in the formed MONT (Φ_1) is accomplished with **Equation 3**:

$$\emptyset_1 = \frac{SLD\ of\ MONT_{experimental} - SLD\ of\ protonated\ MONT_{100p-L1}}{SLD\ of\ deuterated\ MONT_{theoretical} - SLD\ of\ protonated\ MONT_{100p-L1}} \qquad \mathbf{3}$$

In **Equation 3**, the SLD of the protonated MONT at 0 hr. and 10 hrs. is obtained from the fitting of the scattering profile of the MONT formed from the 100 **L1**: 0 **L1-*d*$_8$** mixture, the SLD of deuterated MONT is estimated by assuming there is a similar amount of solvent incorporated into the 100 **L1** MONT structure and that the SLD of $MONT_{experimental}$ is obtained from the fitting of the scattering profile of the MONTs formed from the 80:20, 40:60 and 60:40 **L1**: **L1-*d*$_8$** feeds. **Table 1** reports the volume fraction Φ_1 of the deuterated ligand incorporated into nanostructure formed from the various **L1** and **L1-*d*$_8$** mixtures that are used as the feed.

Table 1. Volume fractions of deuterated **L1** ligand in the MONT structure at 0 hr. and 10hr in the MONTs formed from 80:20, 40:60 and 60:40 **L1** and **L1-*d*$_8$** mixtures.

L1: **L1-*d*$_8$**	Φ_1 (Lamellae) 0 hr. ± error	Φ_1 (Lamellae) 10 hrs. ± error	Φ_1 (Parallelepiped) 0 hr. ± error	Φ_1 (Parallelepiped) 10 hr. ± error
80:20	0.21 ± 0.02	0.21 ± 0.02	0.19 ± 0.01	0.19 ± 0.02
60:40	0.41 ± 0.02	0.41 ± 0.02	0.38 ± 0.01	0.37 ± 0.02
40:60	0.60 ± 0.01	0.60 ± 0.02	0.60 ± 0.02	0.59 ± 0.02

The estimated amount of deuterated ligand in the MONT structures calculated using **Equation 3** shows that final structures formed from the reaction of the ligand **L1** and salt consists of ~20%, ~40% and ~60% deuterated **L1**, which is nearly equal to the amount of deuterated **L1** in the feed at the beginning of the reaction. Therefore, this quantification of amount of deuterated ligand in the final nanostructures formed from the protonated and deuterated **L1** ligands mixtures clearly indicates that the deuterated ligand is randomly distributed in the MONT structure. Correlating the random distribution of deuterated ligands to the reactivity of the two ligands indicates that the protonated and deuterated ligands have similar reactivity in the MONT formation reaction. In other words, similar to a copolymerization reaction where two monomers form a single polymer chain, the metal salt reacts with both protonated and deuterated ligand at the same rate to form a final MONT structure that incorporates both protonated and deuterated ligands in a random manner.

A similar experiment and analysis was also completed to investigate the relative reactivity of the **L1** and **L2** ligands. This is accomplished by determining the amount of deuterated MONT (Φ_1) in the final nanostructure that is formed from mixtures of protonated:deuterated **L1** and **L2**.

To quantify the amount of deuterated MONT formed in this reaction, **Equation 4** is used, which establishes the relationship between the volume fraction of deuterated MONT (Φ_1) and the experimentally determined SLD of the MONT from the SANS profiles:

$$\emptyset_1 = \frac{SLD\ of\ nanostructre_{experimental} - SLD\ of\ protonated\ nanostrucure_{p-L1:p-L2}}{SLD\ of\ deuterated\ MONT_{theoretical} - SLD\ of\ protonated\ nanstrucure_{p-L1:p-L2}} \qquad \mathbf{4}$$

In **Equation 4**, the SLD of the nanostructure at 0 hr. and 10 hrs. reaction time is obtained from the fitting the scattering profile of 50 **L1**:50 **L2**, the SLD of deuterated MONT is determined assuming that there is a the similar amount of solvent incorporated into these MONTs as is found in the 100 **L1** MONT structure and SLD of $nanostructure_{experimental}$ is the SLDs obtained from fitting of the 35:15:50, 25:25:50, 15:35:50, 0:50:50 **L1**: **L1-*d*$_8$**: **L2** scattering profiles. **Table 2** reports the volume fraction Φ_1 of the deuterated nanotube incorporated into the nanostructure formed from mixtures of the **L1**, **L1-*d*$_8$** and **L2** ligands.

Table 2. Volume fractions of deuterated **L1** ligand in MONT structure at 0 hr. and 10hr formed from the 35:15:50, 25:25:50, 15:35:50, 0:50:50 **L1**, **L1-*d*$_8$** and **L2** mixtures.

L1: **L1-*d*$_8$**: **L2**	Φ_1 (Lamellae) 0 hr. ± error	Φ_1 (Lamellae) 10 hrs. ± error	Φ_1 (Parallelepiped) 0 hr. ± error	Φ_1 (Parallelepiped) 10 hr. ± error
35:15:50	0.16 ± 0.02	0.14 ± 0.02	0.15 ± 0.02	0.13 ± 0.02
25:25:50	0.25 ± 0.01	0.23 ± 0.01	0.26 ± 0.01	0.25 ± 0.02
15:35:50	0.35 ± 0.01	0.32 ± 0.02	0.35 ± 0.02	0.33 ± 0.02
0:50:50	0.49 ± 0.01	0.47 ± 0.01	0.46 ± 0.01	0.49 ± 0.02

The estimated amount of deuterated MONT structure determined from this analysis indicates that final structures formed from the reaction of the **L1** and **L2** ligand and the salt consists of ~15%, ~25%, ~35% and ~50% deuterated MONT, values that are very close to the feed of **L1-**

d_8 fed into the reaction. This analysis clearly shows that the MONT formed from the salt and ligands **L1** and **L2** follows a random copolymerization process where the deuterated **L1** ligands are randomly distributed in the copolymeric MONT formed from **L1** and **L2**.

Ligand incorporation in the bulk material was corroborated by ^{1}H NMR analysis of acid-digested MONTs containing the same reaction feed ratios of **L1** : **L1-*d_8*** : **L2** as in **Table 2**. The methylene protons of **L1** and **L2** were integrated against each other with the benzylic proton signal as an internal standard because these positions are stable under both MONT formation and acid digestion. While this bulk analysis cannot show the method of copolymerization, the initial ligand stoichiometric ratios were shown to have close agreement (within 5%) to the acid-digested MONTs (**Figure S5**).

This further indicates that the reactivity of the two ligands (**L1** and **L2**) in this reaction are similar, and thus have a 'reactivity ratio' that is close to 1. This is consistent with a previous study by Barrett et al. that investigated the copolymerization of an **L1**-like ligand with a fluorine-tagged analog, which also showed the random incorporation of its ligands into the final MONT structure.[6] Thus, careful analysis and taking advantage of the ability to tune the contrast variation in small angle neutron scattering offers insight into the relative reactivities of the **L1** and **L2** ligands in their reaction with Cu to form MONT structures. These experiments show that the pair of protonated and deuterated **L1** ligands have similar reactivity in the MONT synthesis reaction, while a similar analysis shows that the reactivity of the **L1** and **L2** ligands are also similar. Thus, the copolymerization of deuterated **L1**, protonated **L1** and **L2** will form MONTs where all three ligands are relatively evenly distributed along the MONTs.

Conclusion

Small angle neutron scattering studies investigate the relative reactivity of 1,2,4-ditriazole-based ligands **L1** and **L2** in the synthesis of MONTs. Monitoring the incorporation of deuterated ligands in the synthesized MONT from a mixed reaction feed provides insight into the relative reactivity of the various ligands. Moreover, careful analysis of the SANS data clearly shows that the formed MONT contains significant solvent within the synthesized nanoscale structure. Quantifying the amount of solvent shows that ca. 45-55% solvent is incorporated into the pores of the nanostructure synthesized from pure **L1** ligands or the mixture of **L1** and **L2** ligands. Our analysis also shows that the MONTs synthesized from pure **L1** ligand form small parallelepiped shaped nanostructures that aggregate and expand in two dimensions to form larger lamellae like MONTs.

Furthermore, the nanostructures formed from a mixture of **L1** and **L2** ligand are of similar size and shape to those formed from the pure **L1** ligand emphasizing the importance of the **L1** ligand in this assembly, suggesting that the presence of the **L1** ligand drives the synthetic process. Finally, correlating the amount of deuterated ligand in the final MONT to the composition of the reaction feed shows that the reactivity of the deuterated **L1** ligand, the protonated **L1** ligand, and the protonated **L2** ligand are very similar and are thus randomly distributed in the synthesized MONT, corroborating prior studies.[6, 17] Thus, this fundamental understanding offers crucial insight to rationally design nanostructures tagged with specific functional groups that will be essential for future MONT/MOF based applications.

Author contributions

J.A.B. and X.B.C. performed ligand synthesis and characterization. J.A.B. conducted PXRD and acid digestion experiments on MONTs and MOFs. M.A.H. and M.D.D performed the neutron

scattering experiments and analyses. M.D.D. and D.M.J. designed and supervised the project. M.A.H., J.A.B., D.M.J., and M.D.D. wrote the paper with input from all authors.

Conflicts of interest

There are no conflicts of interest to declare.

Acknowledgment

J.A.B. and D.M.J. thank the National Science Foundation (NSF DMR 2207224) and the University of Tennessee for support. Research supported as part of the Breakthrough Electrolytes for Energy Storage (BEES), an Energy Frontier Research Center funded by the U.S. Department of Energy (DOE), Office of Science, Basic Energy Sciences (BES), under Award DE-SC0019409 (neutron scattering experiments and analysis). A portion of this research was also completed at the High Flux Isotope Reactor a DOE Office of Science User Facility operated by the Oak Ridge National Laboratory. This work benefited from the use of the SasView application, originally developed under NSF award DMR-0520547. SasView contains code developed with funding from the European Union's Horizon 2020 research and innovation program under the SINE2020 project, grant agreement No 654000.

References

1. Fu, Q.; Lu, Y.; Sun, X.; Wang, X.; Ai, S.-y.; Zhao, R.-S. Recent advances and applications of metal-organic nanotubes in separation and sensor detection science. *TrAC Trends in Analytical Chemistry* **2023**, *163*, 117052.
2. Jia, J.-G.; Zheng, L.-M. Metal-organic nanotubes: Designs, structures and functions. *Coordination Chemistry Reviews* **2020**, *403*, 213083.
3. Eddaoudi, M.; Kim, J.; Rosi, N.; Vodak, D.; Wachter, J.; O'Keeffe, M.; Yaghi, O. M. Systematic Design of Pore Size and Functionality in Isoreticular MOFs and Their Application in Methane Storage. *Science* **2002**, *295* (5554), 469-472.
4. Deng, H.; Doonan, C. J.; Furukawa, H.; Ferreira, R. B.; Towne, J.; Knobler, C. B.; Wang, B.; Yaghi, O. M. Multiple Functional Groups of Varying Ratios in Metal-Organic Frameworks. *Science* **2010**, *327* (5967), 846-850.
5. Ashworth, D. J.; Foster, J. A. Blending functionalised ligands to form multivariate metal–organic framework nanosheets (MTV-MONs) with tuneable surface chemistry. *Nanoscale* **2020**, *12* (14), 7986-7994.
6. Barrett, J. A.; Rosenmann, N. D.; Gnanasekaran, K.; Carroll, X. B.; Gianneschi, N. C.; Jenkins, D. M. Statistical copolymer metal organic nanotubes. *Chemical Science* **2023**, *14* (4), 1003-1009.
7. Dresselhaus, M. S.; Lin, Y. M.; Rabin, O.; Jorio, A.; Souza Filho, A. G.; Pimenta, M. A.; Saito, R.; Samsonidze, G. G.; Dresselhaus, G. Nanowires and nanotubes. *Materials Science and Engineering C* **2003**, *23* (1-2), 129-140.
8. Vailonis, K. M.; Gnanasekaran, K.; Powers, X. B.; Gianneschi, N. C.; Jenkins, D. M. Elucidating the Growth of Metal-Organic Nanotubes Combining Isoreticular Synthesis with Liquid-Cell Transmission Electron Microscopy. *Journal of the American Chemical Society* **2019**, *141* (26), 10177-10182.
9. Zhao, Y.-W.; Zhang, X.-M. The construction of helicate metal–organic nanotubes and enantioselective recognition. *Journal of Materials Chemistry C* **2020**, *8* (13), 4453-4460.
10. Lin, Q.; Ye, Y.; Liu, L.; Yao, Z.; Li, Z.; Wang, L.; Liu, C.; Zhang, Z.; Xiang, S. High proton conductivity in metalloring-cluster based metal-organic nanotubes. *Nano Research* **2021**, *14* (2), 387-391.
11. Rani, D.; Singh, A.; Ladhi, R.; Singla, L.; Choudhury, A. R.; Bhasin, K. K.; Bera, C.; Singh, M. Nanochannel Mediated Electrical and Photoconductivity of Metal Organic Nanotubes. *ACS Sustainable Chemistry & Engineering* **2022**, *10* (21), 6981-6987.
12. Murdock, C. R.; Jenkins, D. M. Isostructural synthesis of porous metal-organic nanotubes. *Journal of the American Chemical Society* **2014**, *136* (31), 10983-10988.
13. Baughman, R. H.; Zakhidov, A. A.; De Heer, W. A. Carbon nanotubes - The route toward applications. *Science* **2002**, *297*, 787-792.
14. Dodson, R. A.; Kalenak, A. P.; Matzger, A. J. Solvent Choice in Metal-Organic Framework Linker Exchange Permits Microstructural Control. *Journal of the American Chemical Society* **2020**, *142* (49), 20806-20813.
15. Falcao, E. H. L.; Wudl, F. Carbon allotropes: beyond graphite and diamond. *Journal of Chemical Technology & Biotechnology* **2007**, *82* (6), 524-531.
16. Rosenmann, N. D.; Barrett, J. A.; Su, S.; Gianneschi, N. C.; Jenkins, D. M. Solvent-Assisted Control of Metal–Organic Nanotube Size and Morphology. *Inorganic Chemistry* **2024**, *63* (19), 8816-8821.

17. Shrestha, U. M.; Vailonis, K. M.; Jenkins, D. M.; Dadmun, M. D. Investigating the Copolymerization of Ligands into Metal-Organic Nanotubes Using Small-Angle Neutron Scattering: Implications for Nanostraws. *ACS Applied Nano Materials* **2020**, *3* (6), 5605-5611.
18. Vailonis, K. M.; Gnanasekaran, K.; Powers, X. B.; Gianneschi, N. C.; Jenkins, D. M. Elucidating the Growth of Metal–Organic Nanotubes Combining Isoreticular Synthesis with Liquid-Cell Transmission Electron Microscopy. *Journal of the American Chemical Society* **2019**, *141* (26), 10177-10182.
19. Etampawala, T.; Mull, D. L.; Keum, J. K.; Jenkins, D. M.; Dadmun, M. Insights into the Morphology and Kinetics of Growth of Silver Metal–Organic Nanotubes. *Crystal Growth & Design* **2016**, *16* (3), 1395-1403.
20. Hammouda, B. *PROBING NANOSCALE STRUCTURES – THE SANS TOOLBOX*; 2008.
21. Roe, R. J. *METHODS OF X-RAY AND NEUTRON SCATTERING IN POLYMER SCIENCE*; TOPICS IN POLYMER SCIENCE; Oxford University Press, Inc., 2000.
22. Nayuk, R.; Zacher, D.; Schweins, R.; Wiktor, C.; Fischer, R. A.; Van Tendeloo, G.; Huber, K. Modulated formation of MOF-5 nanoparticles-A SANS analysis. *Journal of Physical Chemistry C* **2012**, *116* (10), 6127-6135.
23. Lodge, T. P.; Hiemenz, P. C. *Polymer Chemistry*; CRC Press, 2020.
24. *SasView - Small Angle Scattering Analysis*. https://www.sasview.org/ (accessed 2021 December 8).
25. Sears, V. F. Neutron scattering lengths and cross sections. *Neutron News* **1992**, *3* (3), 26-37.

Data Availability Statement

- The data supporting this article have been included as part of the Supplementary Information.